MAKARA, TEKNOLOGI, VOL. 16, NO. 2, NOVEMBER 2012: 144-148

OBSERVATION OF CENTER DISASTER DAMAGE ON PARIAMAN AND WASIOR USING DIFFERENTIAL SAR INTERFEROMETRY (DInSAR)

Dodi Sudiana[*)] and Mia Rizkinia

Department of Electrical Engineering, Faculty of Engineering, Universitas Indonesia, Depok 16424, Indonesia

[*)]*E-mail : dodi.sudiana@ui.ac.id*

Abstract

This study focuses on disaster observations in Pariaman (West Sumatera) and Wasior (Papua) using remote sensing techniques (differential SAR interferometry). Differential interferometry (DInSAR) method was performed on two PALSAR data sets with different acquisition months, i.e. about a month after and before disaster, respectively. The center damage of Pariaman earthquake and Wasior flood can be determined by deriving Land Subsidence using DInSAR method.

Abstrak

Pengamatan Pusat Kerusakan Akibat Bencana Alam di Pariaman dan Wasior Menggunakan *Differential* SAR *Interferometry* (DInSAR). Penelitian ini difokuskan untuk mengamati bencana alam yang terjadi di Pariaman (Sumatera Barat) dan Wasior (Papua) menggunakan teknik-teknik penginderaan jauh (*differential* SAR *interferometry*). Metode DInSAR diterapkan pada dua data PALSAR yang diakuisisi pada bulan yang berbeda, yaitu sekitar sebulan sebelum dan setelah terjadinya bencana. Dengan menganalisis penurunan muka tanah (*land subsidence*) menggunakan metode ini dapat diketahui pusat bencana yang terjadi akibat gempa bumi di Pariaman dan banjir lumpur di Wasior.

Keywords: ALOS/PALSAR, DInSAR, flood potential area, land Subsidence (LS), log ratio

1. Introduction

Earthquakes and landslides are common disturbance in tropical mountainous areas [1–3]. Due to specific geological and climatic conditions, landslide is the most frequent natural disasters after flood in Indonesia, where the percentage of both disasters reached 60 percent, as recorded by the National Disaster Management Agency [4]. Several large landslides (up to several square kilometers) in the world severely affect infrastructures (especially roads) and habitations. The Wasior flood and landslide in Papua, Indonesia, were monitored by PALSAR data before and after the disaster in July 2010 and October 2010, respectively, as well as Pariaman earthquake in September 2009 and October 2009. Based on images generated by DInSAR method for those disasters, both disasters are a serious hazard for inhabited sectors, and it could have impacted buildings, roads and population.

Nowadays, most of the techniques for monitoring landslide and earthquake displacements are derived from measurements from ground based reference stations. Conventional geodetic (i.e., triangulation, tachometry) and also extensometry techniques are the most widely used [5], along with GPS surveys [6–8]. The data acquired using these techniques are available only for major landslides and are limited to several years only. Moreover, the accuracy measurement of these techniques is limited due to the spatial and temporal heterogeneities of ground displacements, such as ground-based measurements. These techniques also require additional human intervention on the landslide.

On the other hand, because it offers a synoptic view of the landslide, remote sensing technique provides a powerful tool to measure landslide displacements that can be repeated at different time intervals. Remote sensing techniques, such as differential SAR interferometry (DInSAR), provide a way to investigate the ground displacement events based on an existing image archive. Previous studies on landslide have been carried out in the C-band and the L-Band in an Alpine context [9–11]. These studies have already showed the center of damage disaster for DInSAR to give a synoptic view of the displacement.

In order to investigate the ground displacement of earthquake and landslide, land subsidence (LS) phenomenon investigated from SAR (Synthetic Aperture Radar) data using Interferometry Approach (InSAR) and Differential Interferometry Approach (DInSAR) can be viewed as one factor and also a parameter indication. DInSAR has an advantage that the number of SAR images required is less with the acquisition of spatially point diverse. It also shows a good level of coherence on the entire set of interferogram [12]. Interferometry generated by a PALSAR L-band data are also has an advantage related to phase unwrapping which often be a problem in SAR interferometry data in C-band wavelength like European Remote Sensing Satellite (ERS). Interferometry of L-band SAR is an appropriate method to monitor the LS in Japan [13]. The output of this research is DInSAR images for center damage in Pariaman earthquake and Wasior landslide.

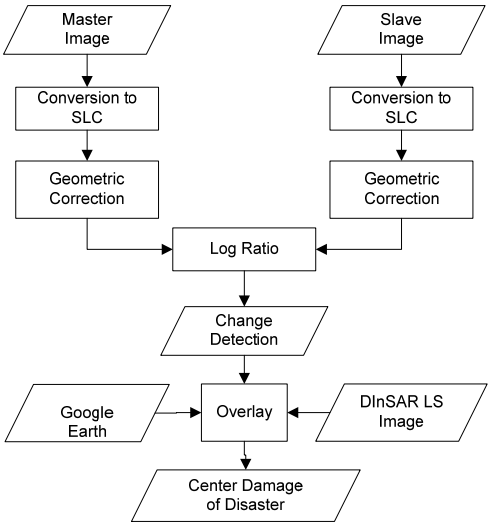

Figure 1. Flowchart of Data Processing ALOS/PALSAR for Observing Center Damage of Disaster

2. Methods

To get the relations between LS and disaster area, we overlaid three images. The first image is the image processing of DInSAR from two Level 1.0 PALSAR data, which cover Wasior and Pariaman in different acquisition months. Each intensity of the image pixel represented in RGB format contains a correlation with phase change. The value of phase change is then converted to an altitude. Thus, from this process, the height change of each pixel could be derived.

The second layer is the image from processing of two data using the Log Ratio method. This method could be used to detect land elevation changes involving statistical values of the image histogram. The results are black and white images that define the area of changes. The third layer is Google Earth images of Pariaman and Wasior in 2010. All data are processed and analyzed systematically as shown in Fig. 1.

Master and slave images are PALSAR imageries taken before and after disaster, respectively, and then they are converted into Single Look Complex (SLC) data. Since the satellite data has disturbed due to satellite height, rotation and roundness of the Earth, it has to be corrected geometrically based on real geographic positions in the surface. Two methods are applied to retrieve the elevation changes using Log ratio and DInSAR, respectively. Log ratio method is implemented to observe where elevation changes occurred, while DInSAR is used to generate the LS map. These results along with the Pariaman and Wasior map in Google Earth are then overlaid to observe the center damage of disaster.

Change detection using log ratio method. Rationalization method minimizes errors in image regions with high intensity, rather than pixel-per-pixel difference that reduces the image intensity values. This is logical since rationalization involves mean and variance of image histogram, which covers the overall pixel values. The log ratio process begins by calculating log ratio detector as the logarithm of the average intensity ratio [14].

If there are two SAR images, $I_1=\{I_1(i, j), 1 \le i \le nrows, 1 \le j \le ncolums\}$ and $I_2 = \{ I_2(i, j), 1 \le i \le nrows, 1 \le j \le ncolumns\}$, thus the *log ratio detector* is defined by [14] as formulated in Eq. (1).

$$I_{LR} = \left[\frac{\sum_{(k.l) \in V_{ij}} I_2(k,l)}{\sum_{(k.l) \in V_{ij}} I_1(k,l)} \right] \quad (1)$$

where V_{ij} is a neighbour pixels (i, j).

To distinguish the changed region (c) from the unchanged (u), a threshold selection criteria is needed. Assuming that c and u in the image ratio (the log ratio results) represented two opposite classes, the minimum error threshold or also called threshold selection criteria Kittler Illingworth (KI) [15], is derived from the assumption that the object and background are normally distributed. KI method is based on Bayesian decision theory and requires a parametric model to describe the statistical distribution for the region that has changed or not [14].

If each of the two components is normally distributed, the criterion function of the KI method is formulated in Eq. (2).

$$J(T) = 1 + 2[P_1(T)\log\sigma_1(T) + P_2(T)\log\sigma_2(T)] - 2[P_1(T)\log P_1(T) + P_2(T)\log P_2(T)] \quad (2)$$

Above parameters can be calculated by Eqs. (3) and (4).

$$P_u(T) = \sum_{g=0}^{T} H(g) \quad \mu_u = \frac{1}{P_u(T)} \sum_{g=0}^{T} H(g)g$$
$$\sigma_u^2 = \frac{1}{p_u(T)} \sum_{g=T+1}^{T} [g - \mu_u(T)]^2 hH(g) \tag{3}$$

$$P_c(T) = \sum_{g=T+1}^{L-1} H(g) \quad \mu_c = \frac{1}{P_c(T)} \sum_{g=T+1}^{L-1} H(g)g$$
$$\sigma_c^2 = \frac{1}{p_c(T)} \sum_{g=T+1}^{L-1} [g - \mu_u(T)]^2 H(g) \tag{4}$$

where H(g) (g = 0,1,..., L-1) is a histogram of the log ratio image. μ_i (T) (i = u,c) is the average value of the class c (changed) and u (unchanged). σ_i^2 (T) (i = u,c) is the variance of both classes. Optimal threshold that minimizes the error is minimized by the function which has the criteria expressed in Eq. (5).

$$T^* = \arg \min_{0 \le T \le L} J(T) \tag{5}$$

Change detection algorithm using log ratio method is intended to help the analysis process by localizing the area of observation height change from PALSAR image. This method is applied to both PALSAR images that has been reconstructed in Single Look Complex (SLC) data. The final step is to compose a color composite image for visualization the phase difference. Basic reduction formula is implemented to retrieve the information value of pixels and phase difference is converted to height difference.

The colors in the image DInSAR results represent different heights. For a single-phase cycle, it represents 2π (pi), where 2π (pi) represents the half of wavelength. Since the wavelength of L-band PALSAR type is 24 cm, a cycle in the image DInSAR could be projected as 12 cm in height.

DInSAR Process. To observe the center of disaster damage, we process the ALOS/PALSAR data using DInSAR algorithm to generate DInSAR image for land subsidence, which is systematically shown in Fig. 2.

The software used for the initial process is PALSAR Processor 2.6.3 and PALSAR Fringe 4.5.1. The earlier software is used to process PALSAR data to retrieve the interferogram. The latter one is then executed to achieve the fringe and color composite which is converted to height as the final result of DInSAR process.

3. Results and Discussion

After making the incision between DInSAR image and log ratio image, the data is presented on a spatial map

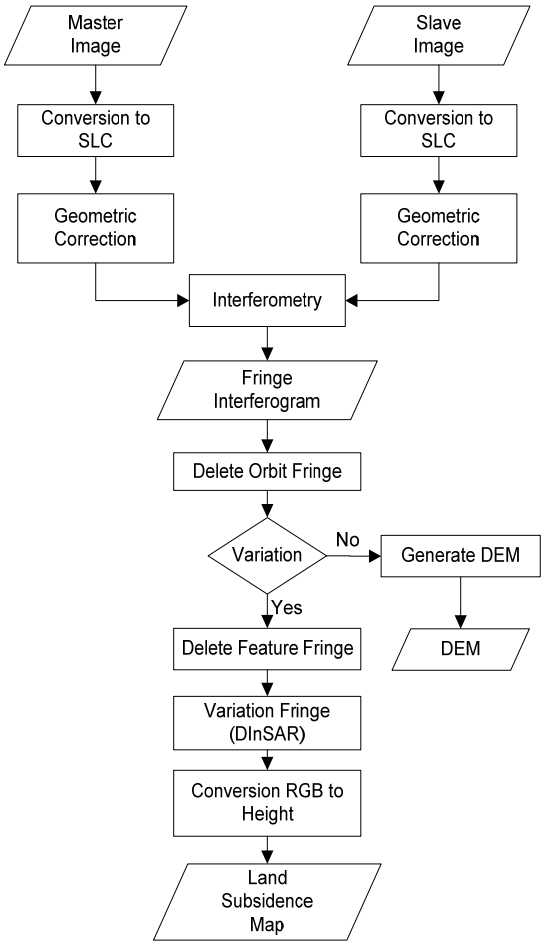

Figure 2. Flowchart of ALOS/PALSAR Data Processing for DInSAR Process

from Google Earth, and overlaid with a map pool. The analysis results showed a color composite of differential fringe in Pariaman as shown in Fig. 3. Based on the map, the center of damage can be determined by observing the fringe pattern which one fringe correspond to a land subsidence of 12 cm in the line of sight on the satellite, shown in Fig. 4.

Fig. 4 showed the differential fringes of Padang Pariaman area. Based on BNPB data [16], Padang Pariaman region is the second largest area impacted by the earthquake after Padang city. The major damage position could be retrieved from the Google Earth in coordinates of E 100”24’ S 0”48’, E 100”22’ S 0”38’, E 100”14’ S 0”34’. As for Wasior, the area covered in the Fig. 6 is the worst impacted area after the flood disaster, which is in accordance with a report in [17].

Furthermore, the color composite of differential fringe in Wasior is shown in Fig. 5. Based on the map, there are four center damages of flood in Wasior (Papua) as shown in Fig. 6.

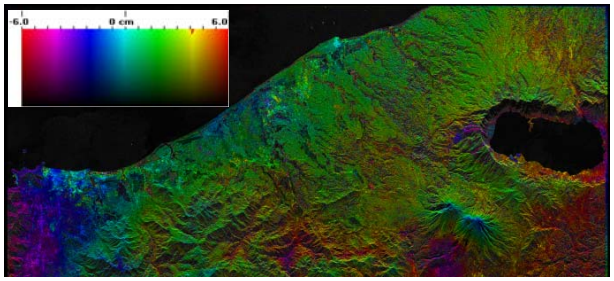

Figure 3. Color Composite of Differential Fringe in Pariaman

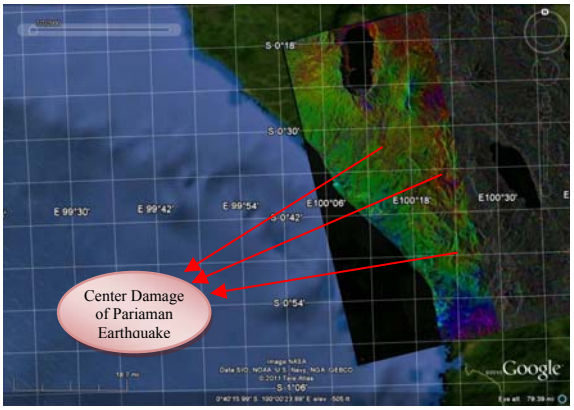

Figure 4. The Center Damage of Pariaman Earthquake by DInSAR Method

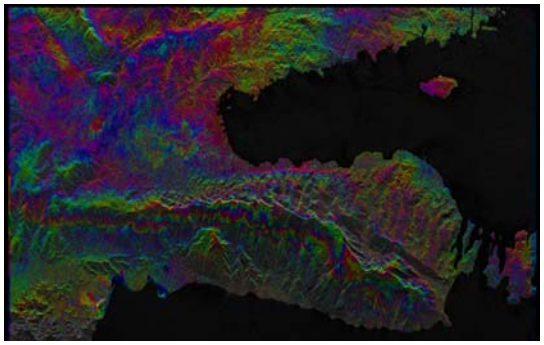

Figure 5. Color Composite of Differential Fringe in Wasior

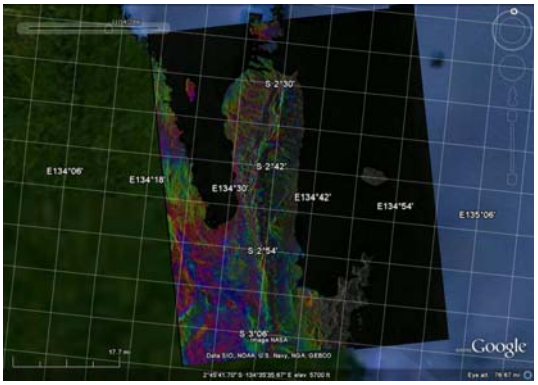

Figure 6. The Center Damage of Wasior Landslide by DInSAR Method

4. Conclusions

Earthquake and flood that happened in Pariaman (West Sumatra) and Wasior (Papua) was also influenced by Land Subsidence (LS). LS value retrieved from ALOS/PALSAR data, using DInSAR method on July and October 2010 for Wasior, and for Pariaman on September and October 2009, have shown the significant changes in elevation. The center damages of Pariaman earthquake and Wasior flood and landslide can be determined by deriving LS using DInSAR method.

Acknowledgment

The authors would like to thank the Microwave Remote Sensing Laboratory (MRSL), Center for Environmental Remote Sensing (CEReS), Chiba University for providing the ALOS/PALSAR images used in this work under the International Collaboration Project funded by the DGHE, Ministry of National Education and the HRKI-UI.

References

[1] C. Restrepo, N. Álvarez, Biotropica 38 (2006) 446.
[2] R.L. Chazdon, Perspectives, Plant Ecol. Evolution Syst. 6 (2003) 51.
[3] F.C. Dai, C.F. Lee, Y.Y. Ngai, Eng. Geol. 64 (2002) 65.
[4] BPBD Nusa Tenggara Timur, Bencana Alam di Indonesia di Dominasi Banjir, *http://www.bpbd.nttprov.go.id/index.php?option=com_content&view=article&id=66:bencana-alam-di-indonesiadidominasibanjir&catid=9: berita-nasional&Itemid=61,* 2010.
[5] M.C. Angeli, A. Pasuto, S. Silvano, A Critical Review of Landslide Monitoring Experiences, Eng. Geol. 55 (2000) 133.
[6] M.E. Jackson, P.W. Bodin, W.Z. Savage, E.M. Nel, U.S. Geol. Surv. Bull. 2130 (1996) 93.
[7] J.P. Malet, O. Maquaire, E. Calais, Geomorphology 43 (2002) 33.
[8] C. Squarzoni, C. Delacourt, P. Allemand, Eng. Geol. 79 (2005) 215.
[9] B. Fruneau, J. Achache, C. Delacourt, Tectonophysics 265 (1996) 181.
[10] C. Carnec, D. Massonnet, C. King, Geophys. Res. Lett. 23 (1996) 3579.
[11] T. Strozzi, U. Wegmuller, C. Werner, A. Wiessmann, V. Spreckels, IEEE. Trans. Geosci. Remote Sens. 41 (2003) 1702.
[12] O. Mora, J.J. Mallorquí, J. Duro, Geosci. Rem. Sens. Symp. IGARSS 4 (2002) 2696.
[13] S. Takeuchi, S. Yamada, Geosci. Rem. Sens. Symp. IGARSS 4 (2002) 2379.

[14] F. Wu, C. Wang, H. Zhang, B. Zhang, Geosci. Rem. Sens. Symp. IGARSS 4 (2007) 2601.
[15] Y. Bazi, L. Bruzzone, F. Melgani, IEEE Trans. on Geosc. Rem. Sens. 43/4 (2005) 874.
[16] Badan Nasional Penanggulangan Bencana (BNPB), Laporan Harian PUSDALOPS BNPB 3 Oktober (2009).
[17] Badan Nasional Penanggulangan Bencana (BNPB), Laporan Harian PUSDALOPS BNPB 13 Oktober (2010).